











## RESEARCH ARTICLE

# Therapeutic effect of paeoniflorin on chronic constriction injury of the sciatic nerve via the inhibition of Schwann cell apoptosis

Di Zhang<sup>1</sup>  | Shiquan Chang<sup>1</sup>  | Xin Li<sup>1</sup>  | Huimei Shi<sup>1</sup>  | Bei Jing<sup>1</sup>  |  
Zhenni Chen<sup>1</sup>  | Yi Lin<sup>1</sup> | Yachun Zheng<sup>1</sup>  | Guoqiang Qian<sup>2</sup>  |  
Yuwei Pan<sup>3</sup>  | Guoping Zhao<sup>1</sup> 

<sup>1</sup>College of Traditional Chinese Medicine, Jinan University, Guangzhou, China

<sup>2</sup>College of Traditional Chinese Medicine, Guangdong Pharmaceutical University, Guangzhou, China

<sup>3</sup>Preventive Treatment of Disease, Tianhe Hospital of Traditional Chinese Medicine, Guangzhou, China

## Correspondence

Guoping Zhao, College of Traditional Chinese Medicine, Jinan University, Guangdong, China.  
Email: [tguo428@jnu.edu.cn](mailto:tguo428@jnu.edu.cn)

Yuwei Pan, Tianhe Hospital of Traditional Chinese Medicine, Guangzhou, China.  
Email: [pywyvette@foxmail.com](mailto:pywyvette@foxmail.com)

## Funding information

National Natural Science Foundation of China, Grant/Award Number: 81874404; TCM Research Project of Guangdong Provincial Bureau of TCM, Grant/Award Number: 20222171; Guangzhou TCM and Integrated Traditional Chinese and Western Medicine Science and Technology Project, Grant/Award Number: 202185151002

## Abstract

Therapeutic drugs of chronic neuralgia have a high risk of addiction, making it crucial to identify novel drugs for chronic neuralgia. This study aimed to explore the therapeutic effect of paeoniflorin on chronic sciatica via inhibiting Schwann cell apoptosis. 28 SD rats were randomly divided into four groups, including the sham operation group, chronic constriction injury (CCI) group, mecobalamin group, and paeoniflorin group. The therapeutic effect and mechanism of paeoniflorin were evaluated via rat and cell experiments. Mechanical, hot, or cold hyperalgesia was induced in the rats after CCI operation, while paeoniflorin relieved chronic neuralgia. Besides, paeoniflorin decreased the levels of IL1, IL6, TNF- $\alpha$ , CRP, and LPS and increased the level of IL10 in serum. As for the sciatic nerve, the number of inflammatory cells was decreased, and Schwann cells were present after paeoniflorin treatment, and paeoniflorin promoted the recovery of nerve structure. In cell experiments, LPS induced Schwann cell apoptosis via the TLR4/NF- $\kappa$ B pathway. And paeoniflorin attenuated LPS-induced Schwann cell apoptosis by decreasing the levels of TLR4, p-NF- $\kappa$ B, caspase3, cleaved-caspase3, and cleaved-caspase7. Overall, these results suggest that paeoniflorin alleviates chronic sciatica by decreasing inflammatory factor levels and promotes the repair of damaged nerves by reducing Schwann cell apoptosis.

## KEYWORDS

chronic constriction injury, chronic neuralgia, paeoniflorin, Schwann cells, sciatica, TLR4/NF- $\kappa$ B

**Abbreviations:** BDNF, Brain-derived neurotrophic factor; CCI, Chronic constriction injury of sciatic nerve; CRP, C-reactive protein; IL1 $\beta$ , Interleukin-1 $\beta$ ; IL6, Interleukin-6; LPS, Lipopolysaccharide; MWT, Mechanical withdrawal threshold; NF- $\kappa$ B, Nuclear factor-kappa B; NGF, Nerve growth factor; PWL, Paw withdrawal latency; SNK, Student-Newman-Keuls; TNF- $\alpha$ , Tumor necrosis factor- $\alpha$ ; TRL4, Toll-like receptor 4.

Di Zhang, Shiquan Chang, and Xin Li contributed equally to this work.

## 1 | INTRODUCTION

Chronic neuropathic pain, which directly results from several diseases that affect the somatosensory system, is a common clinical problem that manifests as increased pain sensitivity (sensitivity to heat, cold

This is an open access article under the terms of the [Creative Commons Attribution-NonCommercial-NoDerivs](https://creativecommons.org/licenses/by-nc-nd/4.0/) License, which permits use and distribution in any medium, provided the original work is properly cited, the use is non-commercial and no modifications or adaptations are made.

© 2022 The Authors. *Phytotherapy Research* published by John Wiley & Sons Ltd.

and mechanical stimuli) (Treede et al., 2008; Truini, Garcia-Larrea, & Cruccu, 2013). As it is difficult to satisfactorily treat neuropathic pain, long-term drug treatment is required, which imposes a burden on the global economy and public health. Now, physicians prescribe drugs such as antipyretic analgesics, opioids, and nonopioids to relieve pain. However, these drugs have a high risk of addiction in patients (Pichini, Solimini, Berretta, Pacifici, & Busardo, 2018), thus making it crucial to identify novel and nonaddictive drugs for the efficacious treatment of chronic neuropathic pain.

The proliferation and migration of Schwann cells in rats after sciatic nerve injury enabled nerve regeneration and substantial functional recovery (Q. Chen, Liu, Zhang, Li, & Yi, 2021). Schwann cells are a dominant glial cell type in the neural system and can promote axonal regeneration (Gonzalez-Perez et al., 2018). After peripheral nerve injury, Schwann cells undergo cell reprogramming during Wallerian degeneration and transform from mature and differentiated myelinating Schwann cells into repair Schwann cells. Furthermore, the proliferation and migration of Schwann cells and inhibition of cell ageing and apoptosis can restore the structure of injured peripheral nerves (Kou et al., 2020).

Paeoniflorin is the active ingredient in a traditional Chinese medicine derived/extracted from the plant *Paeonia lactiflora*, which is used to cure pain (He & Dai, 2011). Paeoniflorin was previously shown to inhibit Schwann cell injury and apoptosis induced by hydrogen peroxide by inhibiting the phosphorylation of p38MAPK and reducing the levels of caspase3, cleaved-caspase3, and cleaved-caspase7 (Zhang, Yang, et al., 2021). Additionally, treatment of neuralgia with paeoniflorin was shown to increase the production of nerve growth factor (NGF) and brain-derived neurotrophic factor (BDNF) through PI3K- and PKA-dependent pathways in rat glial cells (Guo et al., 2020). Paeoniflorin reversed the neurotoxicity produced by corticosterone and may exert a neuroprotective effect by promoting the phosphorylation of Akt (Yuan et al., 2020). In summary, paeoniflorin has strong neuroprotective properties (Tao et al., 2017). Paeoniflorin was previously shown to reduce the responses of astrocytes and microglia to injury (D. Zhou et al., 2019), to elevate the expression levels of p-p38 MAPK and NF- $\kappa$ B in the spinal cord (J. Zhou et al., 2017), and to decrease the expression of IL-1 $\beta$  and TNF- $\alpha$ , indicating that it can attenuate neuroinflammation.

This study aims to find the therapeutic effect and mechanism of paeoniflorin in the treatment of chronic neuralgia. Now, we first examine the therapeutic effect of paeoniflorin on chronic constriction injury (CCI) of the sciatic nerve via behavioral tests, pathological examination, and immunohistochemistry. Next, we investigate the underlying mechanism at the cellular level to provide additional experimental evidence supporting the use of paeoniflorin for the treatment of nerve injury.

## 2 | MATERIALS AND METHODS

### 2.1 | Subjects

Twenty-eight male Sprague–Dawley rats (SD rats) weighing approximately 200–230 g and aged 7–8 weeks were acquired from the

experimental center of Beijing Huafukang Co. Ltd. These rats were housed at 5 animals per cage at the Animal Experimental Centre of the Medical College of Jinan University. All animal experiments were conducted in accordance with guidelines established by the National Academy of Sciences, the National Institutes of Health (NIH) (Institute of Laboratory Animal Resources (U.S.). Committee on Care and Use of Laboratory Animals.) and in accordance with the guidelines of Animal Ethical Committee of Jinan University (ethics approval number: 20181008-04).

### 2.2 | Reagents

Paeoniflorin (S31585; 97% purity) was acquired from Guangzhou Jiayan Co. Ltd. Mecobalamin (production lot number: 1703098) was purchased from Eisai Pharmaceutical Co., Ltd. The Cell Counting Kit-8 (96992) and Annexin V FITC Apoptosis Detection Kit I (556547) were obtained from Guangzhou Juyan Biological Co., Ltd. IL1 $\beta$ , IL6, TNF- $\alpha$ , CRP, lipopolysaccharide (LPS), and IL10 ELISA kits (MM-0047R1, MM-0190R1, MM-0180R1, MM-0081R1, MM-0647R1, and MM-0195R1, respectively) were purchased from Jiangsu MEIMIAN Industrial Co., Ltd. LPS (L2880), TAK-242 (S80562, a TLR4 inhibitor), and JSH23 (M134534; a NF- $\kappa$ B inhibitor) were acquired from Guangzhou Yiyou Biotechnology Biological Co., Ltd. The phosphatase inhibitor cocktail 1 (RBG2012) and BCA protein content kit (P0010S) were acquired from Guangzhou Junji Biotechnology Co., Ltd. PageRuler Prestained Protein Ladder and Marker (P12083) was obtained from Shanghai Bioscience Technology Co., Ltd. (China). The SYBR Green Premix qPCR kit for RT-PCR, and RNase-free water (AG11701, AG11602, and AG11012, respectively) were obtained from Accurate Biotechnology Co., Ltd. (Hunan). The rabbit polyclonal Bcl-2, caspase3, cleaved-caspase3, cleaved-caspase7, and  $\beta$ -actin antibodies (ab59348, 9662S, 9664S, 8438S, and 4970S, respectively) were acquired from Guangzhou Juyan Biological Co., Ltd. The polyclonal rat anti-rabbit S100 $\beta$  and NF- $\kappa$ B antibodies (GB13359 and GB11997, respectively) were purchased from Servicebio Co., Ltd. The p-NF- $\kappa$ B and TLR4 antibodies (8690S and 511049, respectively) were acquired from Guangzhou Yiyou Biotechnology Biological Co., Ltd. Schwann cells (RSC96 cells) were acquired from the Shanghai Institute of Cell Biology (GMR6; China). The cell line used in the experiments was between passages 6 and 10.

### 2.3 | Neuropathic pain model

We generated a CCI sciatic nerve model according to previous studies (Yoon, Wook, Sik, Ho, & Mo, 1994; Zhang et al., 2020). First, the rats were injected with pentobarbital sodium (3%; 40 mg/kg) and fixed, after which the right sciatic nerve was exposed. The right sciatic nerve was ligated with 4.0 sutures at 4 sites approximately 1 mm apart under a microscope. During this time, we observed a small twitch in the operated hind limb. Next, gentamicin (10 mg/ml, i.m.) was injected into the right biceps femoris. The rats in the sham group were subjected to suturing of the skin and muscles but not nerve ligation.

## 2.4 | Treatment programs

Twenty-eight rats were randomly divided into four groups: the sham operation group, CCI group, mecobalamin group, and paeoniflorin group. After the operations, the rats in the sham operation and CCI groups were administered saline (0.9%; 6 ml/kg/d/bid), the rats in the mecobalamin group were administered mecobalamin (dissolved in saline, 10 mg/kg/d/bid) via gavage based on dose conversion between animals and human (Nair & Jacob, 2016), and the rats in the paeoniflorin group were administered paeoniflorin (dissolved in saline, 10 mg/kg/d/bid) via gavage (Ma et al., 2016). The rats were administered oral medications for 21 days. Mecobalamin can repair and restore the sciatic nerve structure and thus served as a positive drug control.

## 2.5 | Behavioral tests

Behavioral tests include acetone experiment, hot plate experiment, and von Frey test (Zhang et al., 2019). To assess cold hyperalgesia, we chose acetone experiment. 100  $\mu$ l of acetone was dropped on the plantar surface of the right paw. Next, we noted the total number of times that the rat lifted or clutched its right hind paw during 120 s. Thermal hyperalgesia was evaluated by a hot plate experiment (YLS-6B; Jinan Yiyuan Technology Development Co., Ltd.) to measure the paw withdrawal threshold (PWT). The lateral plantar surface was exposed to a heated plate (50°C), and the time to raise the right foot was recorded. The von Frey test was to evaluate mechanical hyperalgesia [50% mechanical withdrawal threshold (MWT)]. The hind paw was stimulated 10 times with each filament (2.0–26.0 g) beginning with the 2-g filament, and paw lifting was considered a positive response. If we detected a positive response, we calculated the pain threshold (50% g threshold =  $10^{[X_f + k\sigma]}/10,000$ ). We assessed hyperalgesia of the right paw on the 1st, 4th, 7th, 14th, and 21st days after surgery. All tests were replicated three times with 10 min intervals for each paw, and the mean was calculated. Behavioral experiments were conducted by a blind observer.

## 2.6 | Hematoxylin-eosin staining and ELISA

The liver, kidney, ligated sciatic nerve tissues were incubated in 4% paraformaldehyde for 1 day, after which they were embedded in paraffin and sectioned at a thickness of 3  $\mu$ m. The sections were deparaffinized by xylene and immersed in 100, 90, 80, and 70% ethanol. Next, we rinsed the sections with PBS for 5 min. After staining, two pathologists who were blinded to the experimental design observed the stained images and assessed tissue damage. Under anaesthesia, we collected 8 ml of blood from the abdominal aorta. The rat serum was centrifuged at 3000 rpm for 15 min at 4°C, and 200  $\mu$ l of the supernatant was retained to measure the levels of inflammatory factors. We diluted the serum 10 times to ensure that the concentration was within the standard curve. The remaining

experimental operations were performed according to the manufacturer's instructions. We used a microplate reader (Bio-Tek Instruments, Inc.) to measure the optical density.

## 2.7 | Immunohistochemistry analysis of the sciatic nerve

The right sciatic nerves (from 3 rats) were fixed in 4% paraformaldehyde for 24 hr. Next, they were transferred to a 20% (w/v) sucrose solution and sectioned at a thickness of 9  $\mu$ m. The sections from individual animals were incubated in sodium citrate antigen repair solution (1:1000 dilution; pH = 6). Next, the sections were incubated with primary antibodies diluted 1:200 and then with the corresponding secondary antibody. The stained sections were viewed under an OLYMPUS fluorescence microscope (BX53). We calculated the IOD/area ratio using Image-Pro Plus software (Media Cybernetics, Inc.) and conducted statistical analysis.

## 2.8 | Cell viability and cytotoxicity assays

The viability of Schwann cells was determined by the CCK-8 assay. Schwann cells were seeded in 96-well plates at a density of  $6 \times 10^3$  cells/well. We examined the effects of different drugs on cell activities. According to the cell viability results, TAK-242, JSH23, and paeoniflorin were used at concentrations of 10  $\mu$ g/ml, 10  $\mu$ M (Y. T. Chen, Wang, et al., 2021), 10  $\mu$ M (Zhai, Liang, & Xu, 2021), and 50  $\mu$ M (Zhang, Yang, et al., 2021), respectively.

## 2.9 | Grouping and drug concentrations for the cell experiment

The experiment was divided into two parts. In the first part, cells were allocated into the control group, LPS group (10  $\mu$ g/ml LPS), TAK-242 group (10  $\mu$ g/ml LPS + 10  $\mu$ M TAK-242), and JSH23 group (10  $\mu$ g/ml LPS + 10  $\mu$ M JSH23). In the second part, cells were allocated into the control group, LPS group (10  $\mu$ g/ml LPS), paeoniflorin group (50  $\mu$ M paeoniflorin), and LPS + paeoniflorin group (10  $\mu$ g/ml LPS + 50  $\mu$ M paeoniflorin). Schwann cells ( $1.2 \times 10^5$  cells/well) were cultured in 6-well plates for 24 hr. Next, the medium was discarded, and the cells were washed with PBS. The drugs and LPS were added to the medium at the same time, followed by culture for 24 hr.

## 2.10 | Hoechst 33258 staining

After drug treatment and LPS cotreatment, the cells were washed with PBS. The cells in each well were then incubated with Hoechst 33258 (5  $\mu$ l in 0.995 ml of PBS) for 20 min. After washing with PBS twice, fluorescence images (three photographs per well) were acquired with an inverted fluorescence microscope. The experiments

**TABLE 1** Primer sequences

Gene	Forward primer (5'-3')	Reverse primer (5'-3')
Bcl-2	CAGGCTGGAAGGAGAAGAT	CGGGAGAACAGGGTATGA
Bcl-xl	TAGGTGGTCATTCAGGTAGG	GTGGAAAGCGTAGACAAGG
IL6	AGTTGCCTTCTGGGACTGATGT	GGTCTGTTGTGGGTGGTATCCTC
TNF- $\alpha$	GCGTGTTTCATCCGTTCTCTACC	TACTTCAGCGTCTCGTGTGTTTCT
IL1 $\beta$	AGGAGAGACAAGCAACGACA	CTTTCCATCTTCTTTGGGTAT
$\beta$ -actin	GAGAGGGAAATCGTGCCT	GGAGGAAGAGGATGCCG

were repeated three times, and the fluorescence intensity was calculated using Image-Pro Plus software.

### 2.11 | Cell apoptosis detection by flow cytometry

Annexin V-FITC and PI staining were conducted to evaluate the rate of Schwann cell death. After treatment, cells were harvested with trypsin and washed with PBS. After that,  $1 \times 10^6$  cells were incubated in binding buffer and double-stained with Annexin V-FITC and PI in the dark for 20 min at 4°C. Next, we analyzed the fluorescence intensity of the cells by flow cytometry (CytExpert 2.3; Beckman Coulter, Inc.).

### 2.12 | Quantitative real-time PCR

According to the manufacturer's instructions, total RNA was harvested using RNAiso Plus and synthesized into cDNA with a RT-PCR kit in accordance with the manufacturer's instructions. The amplification parameters were 95°C for 30 s, followed by 40 cycles of 95°C for 5 s and 60°C for 34 s, 95°C for 15 s, 60°C for 60 s, and 95°C for 15 s. The relative expression of mRNA was calculated by the  $2^{-\Delta\Delta Cq}$  method after normalization to  $\beta$ -actin (Livak & Schmittgen, 2001; Zhang, Sun, et al., 2021). For this procedure, the Applied Biosystems 7900 real-time PCR (qPCR) system was used to conduct qRT-PCR. SYBR<sup>®</sup> Green Premix qPCR, and the primers utilized are shown in Table 1.

### 2.13 | Western blot analysis

The levels of Bcl-2, caspase3, cleaved-caspase3, cleaved-caspase7, TLR4, NF-kB, and p-NF-kB were measured by Western blotting. Total protein was isolated with a protein extraction kit in accordance with the manufacturer's instructions. We determined the protein concentrations using the BCA assay. The proteins (30  $\mu$ g) were separated by 4–10% SDS-PAGE, transferred onto PVDF membranes, blocked with 5% skimmed milk powder for 1 hr, incubated with a primary antibody (1:1000) overnight at 4°C for 24 hr, and incubated with a secondary antibody (1:30000) for 45 min. Finally, chemiluminescence was used to visualize the blots (ChemiDoc XRS). Each experiment was conducted in triplicate.

### 2.14 | Immunofluorescence staining

A slide coated with poly L-lysine (0.1 mg/ml) was placed in a 6-well plate. RSC96 cells were cultured and treated as indicated, fixed with 4% paraformaldehyde for 30 min at room temperature, and permeabilized with 0.3% Triton X-100 for 15 min. After three rinses with PBS, the cells were blocked with 1% bovine serum albumin for 1 hr and then incubated with a rabbit anti-NF-kB p65 primary antibody (1:200 dilutions) at 4°C overnight. The next day, the cells were washed with PBS three times and incubated with a fluorescein isothiocyanate (FITC)-conjugated goat anti-rabbit secondary antibody (1:400 dilutions) for 1 hr at room temperature. The cells were treated with an antifade mounting medium with DAPI for 10 min at 37°C in the dark. All images were captured with a fluorescence microscope (Olympus, Japan) at magnifications of  $\times 200$  and  $\times 400$ .

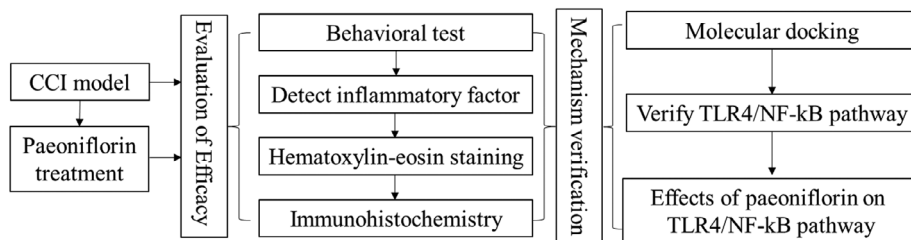
### 2.15 | Validation of the paeoniflorin–TLR4 interaction by molecular docking

To further validate the robust association between paeoniflorin and TLR4, we performed a molecular docking analysis of the two components. First, we acquired the 2D structure of paeoniflorin from PubChem and the 3D protein structure of TLR4 from the RCSB PDB database. PyMOL software was then used to elucidate the original ligand conformation of the target protein. After the ligand and receptor molecule preparation, we conducted molecular docking with Auto Dock vina. After adding the polar hydrogen and Gasteiger charges to the presented receptors and ligands, semiflexible docking was employed. The binding energy ( $< -5.5$ ) was used to evaluate the molecular docking analysis results. Finally, PyMOL software was used to analyze and visualize the docking results of paeoniflorin and TLR4.

### 2.16 | Statistical analyses

We conducted all statistical analyses and generated the graphs with GraphPad Prism 8, Adobe Illustrator 2020, and SPSS 18.0 software. Analyses of the behavioral results were conducted by repeated analysis of variance (ANOVA), and all other data were analyzed by one-way ANOVA. The Student–Newman–Keuls (SNK) post hoc test was performed after ANOVA. In all cases,  $p < .05$  was considered statistically significant.

## 2.17 | Study design



## 3 | RESULTS

### 3.1 | Behavioral results

The rats in the CCI group exhibited cold, mechanical, and thermal hyperalgesia on the 4th day after the operation (Figure 1A-C;  $p < .05$ ). Additionally, these symptoms were more apparent from the fourth day to the 21st day. Treatment with paeoniflorin and mecobalamin (positive drug control) relieved neuropathic pain but did not normalize sensitivity from the 4th day to the 21st day (Figure 1A-C;  $p < .05$ ). The rats in the paeoniflorin group were more sensitive to mechanical, cold, and thermal stimulation than those in the mecobalamin group (7, 14, and 21 days; Figure 1A-C;  $p < .05$ ). The results showed no functional recovery for the constricted sciatic nerves.

### 3.2 | Serum inflammatory factor levels

The expression levels of IL1, IL6, TNF- $\alpha$ , CRP, and LPS were increased sharply in the CCI group, while those of IL10 were decreased (Figure 1D-H,I;  $p < .05$ ). Mecobalamin and paeoniflorin treatment reversed these changes in the serum levels of inflammatory factors (Figure 1D-H,I;  $p < .05$ ). Mecobalamin decreased the levels of TNF- $\alpha$  and LPS to normal levels, while paeoniflorin restored the expression of only LPS to a nearly normal level (Figure 1F,H;  $p < .05$ ).

### 3.3 | Hematoxylin-eosin staining

On the 21st day, we observed the structures of the sciatic nerve, liver, and kidney. Staining (Figure 1J) revealed few Schwann cells and inflammatory cell infiltration in the sham operation group. Obvious inflammatory cell infiltration and Schwann cell proliferation were observed in the CCI, mecobalamin, and paeoniflorin groups. After treatment, the number of inflammatory cells was decreased and Schwann cells were present, but the organizational structure and morphology of the sciatic nerve were not restored to normal in the mecobalamin and paeoniflorin groups. Hematoxylin-eosin staining of liver and kidney samples revealed that the liver and kidney structures were normal in all the groups. Thus, paeoniflorin, mecobalamin, and

CCI did not have negative effects on the livers and kidneys of the rats (Figure 1K,L).

### 3.4 | Immunohistochemistry analysis of the sciatic nerve

Immunohistochemistry staining of the sciatic nerve is shown in Figure 2. In the normal sciatic nerve, Bcl-2 and S100 $\beta$  were distributed in the myelin sheath, which was observed as the tissue structure around the nerve (Figure 2). The sciatic nerve was destroyed in rats undergoing CCI, as indicated by the aberrant distribution of Bcl-2 and S100 $\beta$ . After treatment with paeoniflorin, the sciatic nerve tissue was not restored to normal. Additionally, the levels of Bcl-2 and S100 $\beta$  in the CCI group were lower than those in the other groups (Figure 2A, B;  $p < .05$ ). The levels of caspase3 and TLR4 were higher in the CCI group than in the other groups (Figure 2C,D;  $p < .05$ ). Paeoniflorin and mecobalamin increased the levels of Bcl-2 and S100 $\beta$  and decreased the levels of caspase3 and TLR4 (Figure 2A-D;  $p < .05$ ).

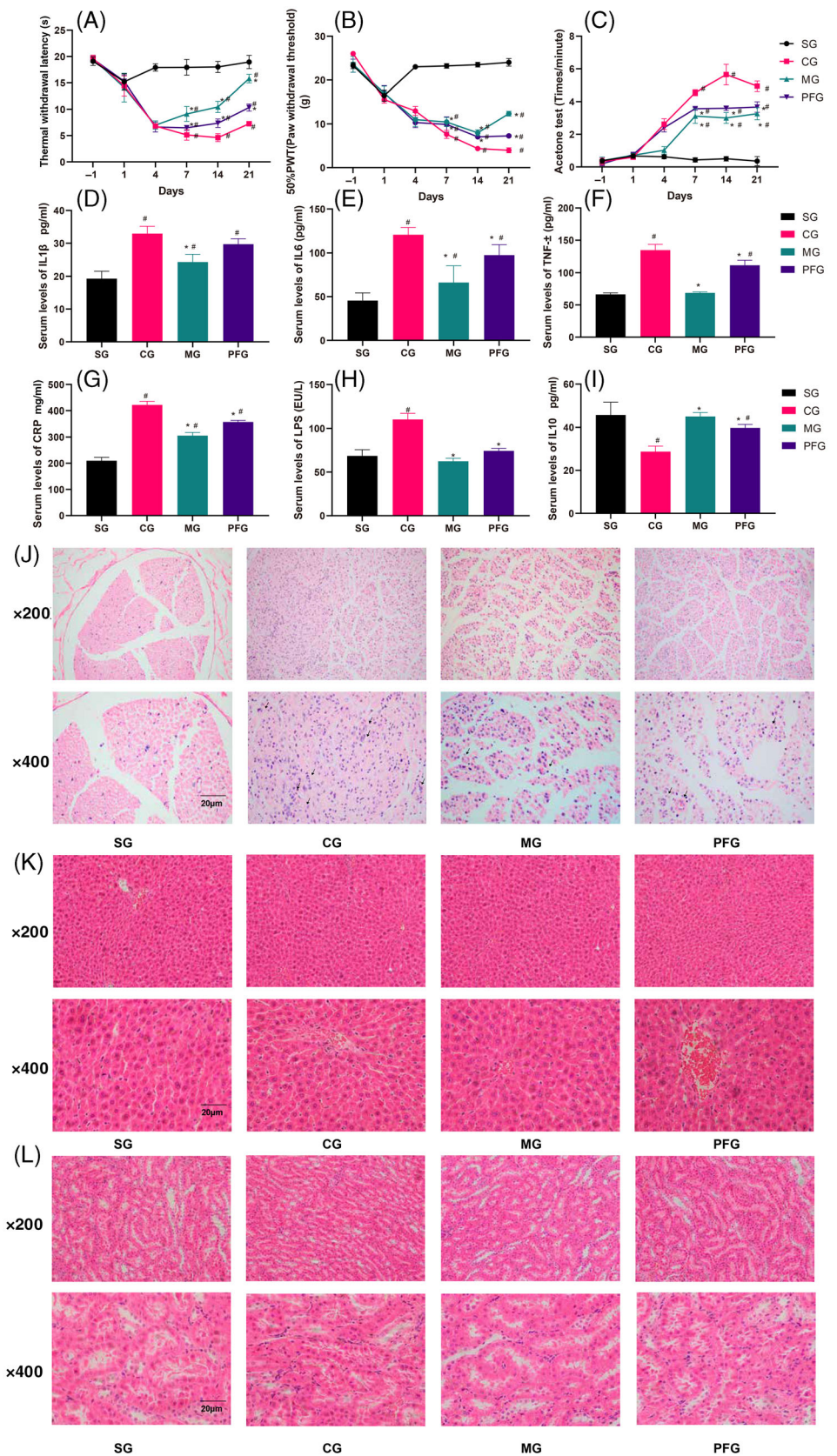
### 3.5 | Hoechst 33258 staining and the mRNA levels of Bcl-2 and Bcl-xl

Hoechst staining of RSC96 cells revealed that LPS induced nuclear apoptosis (Figure 3A), and a TLR4 inhibitor (TAK-242) and NF-kB inhibitor (JSH23) reversed this trend (Figure 3A1;  $p < .05$ ). LPS decreased the mRNA expression of Bcl-2 and Bcl-xl, while TAK-242 and JSH23 had the opposite effect. However, only JSH23 restored the mRNA levels of Bcl-2 and Bcl-xl to normal levels (Figure 3B;  $p < .05$ ).

### 3.6 | Expression of proteins related to apoptosis and the TLR4/NF-kB pathway and the nuclear translocation of NF-kB

In the LPS group, the levels of cleaved-caspase3, caspase3, cleaved-caspase7, p-NF-kB, and TLR4 were obviously increased (Figure 3C;  $p < .05$ ). TAK-242 and JSH23 reduced the expression levels of these

**FIGURE 1** Behavioral results, levels of serum inflammatory factors, and hematoxylin-eosin staining. (A–C) Rat behavioral tests. (D–I) Analyses of serum inflammatory factors. (J) (sciatic nerve), (K) (liver), and (L) (kidney) show pathological staining. #Compared with the sham operation group. \*Compared with the CCI group.  $n = 6$



molecules (Figure 3C;  $p < .05$ ). The expression of NF- $\kappa$ B was nearly equal between the groups. TAK-242 reduced the levels of p-NF- $\kappa$ B and TLR4, while JSH23 decreased the level of only p-NF- $\kappa$ B ( $p < .05$ ).

In the LPS group, the nuclear translocation of NF- $\kappa$ B was clearly observed, and TAK-242 and JSH23 reversed this phenomenon (Figure 3D).

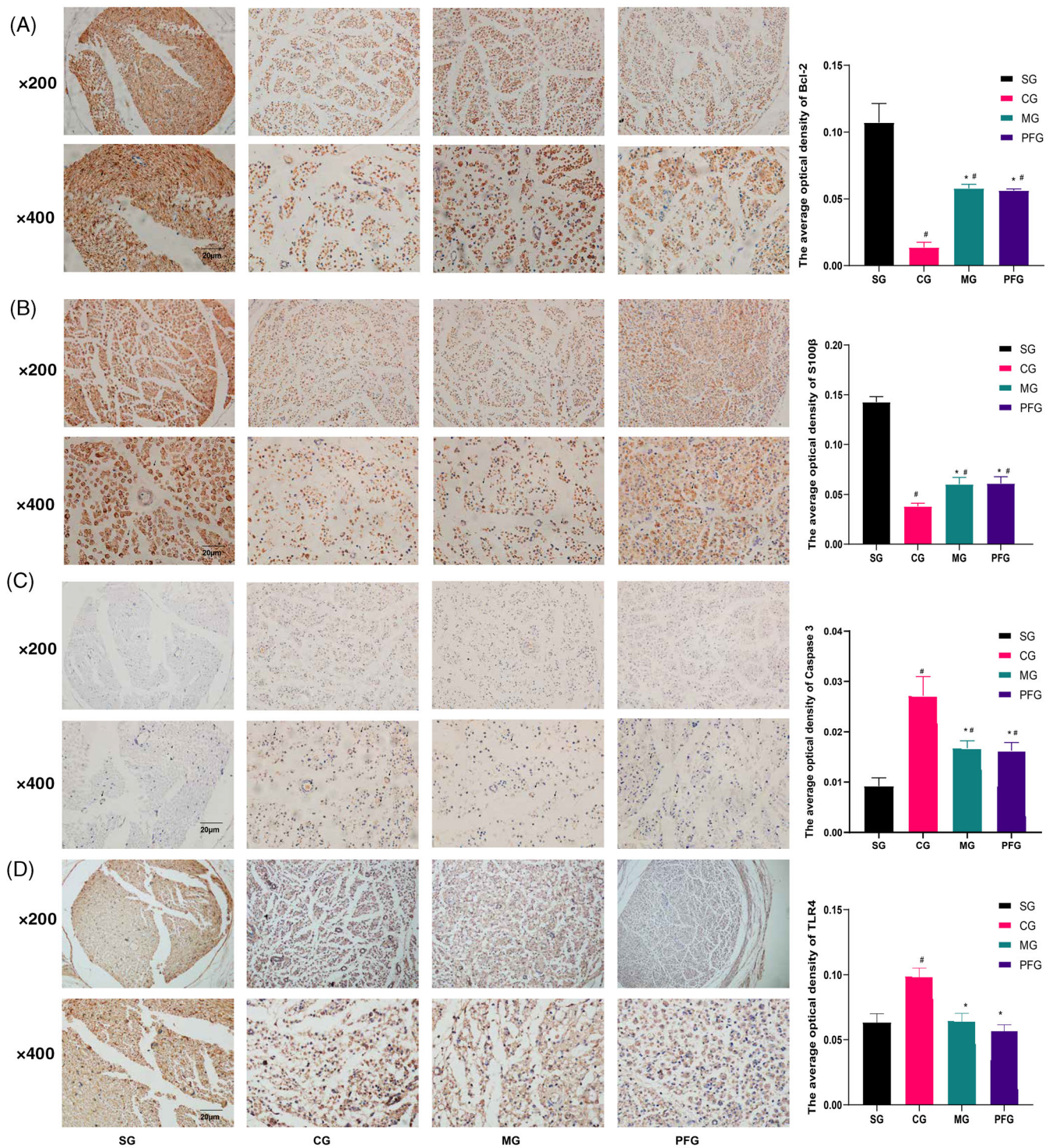


**FIGURE 2** Immunohistochemistry analysis of the sciatic nerve. Distributions of Bcl-2 (A), S100 $\beta$  (B), caspase3 (C), and TLR4 (D) in the sciatic nerve. The nucleus is shown in blue, and the target protein is shown in yellow. <sup>#</sup>Compared with the sham operation group. <sup>\*</sup>Compared with the CCI group.  $n = 3$

### 3.7 | Validation of the paeoniflorin–TLR4 interaction by molecular docking

To further verify the binding capacity between paeoniflorin (Figure 3E) and TLR4, a molecular docking analysis was performed. We acquired

the PDB code (3T6Q) from RCSB and from a previously published study. The binding energy (Figure 3F) of the paeoniflorin–TLR4 interaction indicated good binding activities. The paeoniflorin–TLR4 complex was stabilized by hydrogen bonds with residues that had adhesive lengths of 2.7, 3.0, 3.0, 3.1, 2.9, 2.9, and 3.2 Å (Figure 3F).

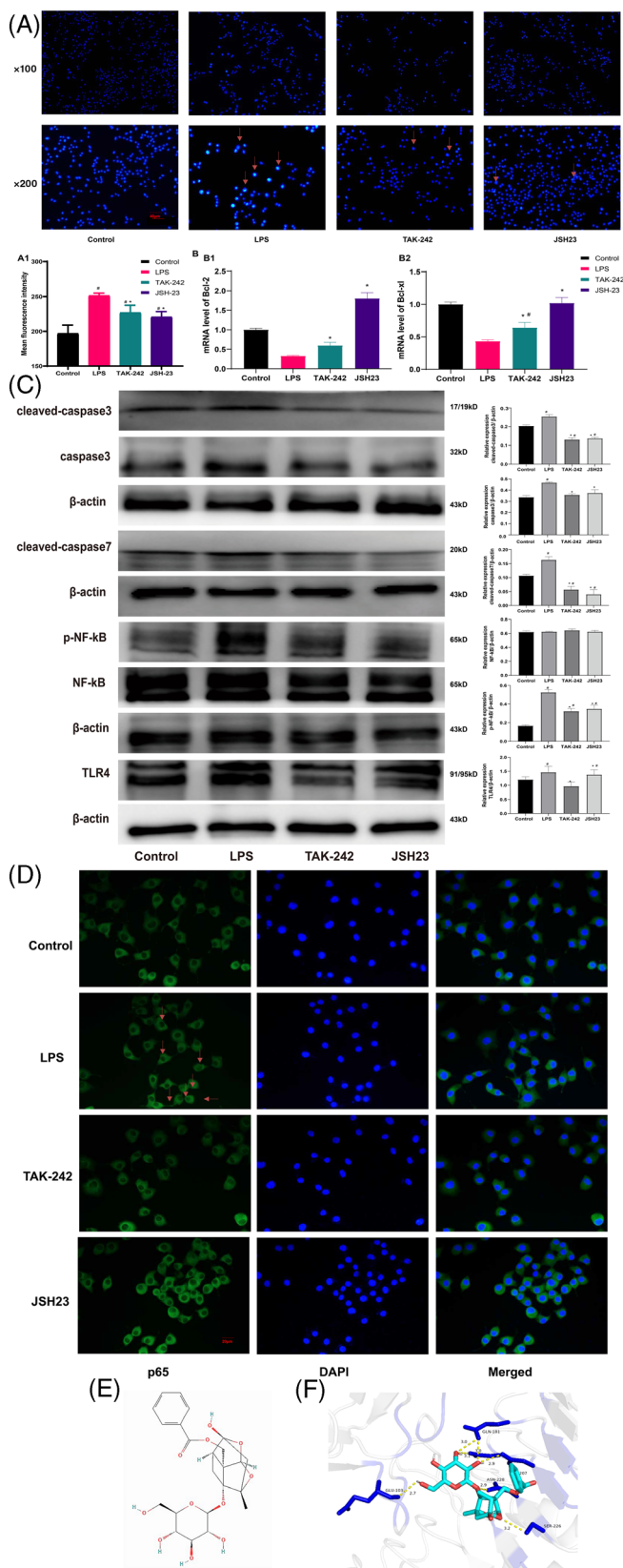


**FIGURE 3** Hoechst staining, mRNA levels of Bcl-2 and Bcl-xl and expression levels of proteins related to apoptosis and the TLR4/NF-κB pathway. (A) Nuclear apoptosis. (B) The mRNA levels of Bcl-2 and Bcl-xl. (C) The expression levels of related proteins. (D) The nuclear translocation of NF-κB. (E) The structure of paeoniflorin. (F) The paeoniflorin-TLR4 interaction. #Compared with the sham operation group. \*Compared with the CCI group.  $n = 3$

### 3.8 | Alleviation of LPS-induced apoptosis by paeoniflorin

Flow cytometry indicated that LPS induced RSC96 cell apoptosis (Figure 4A;  $p < .05$ ), which was confirmed by Hoechst staining (Figure 4B;  $p < .05$ ). Fluorescence intensity was greater in the LPS group than that in the other groups (Figure 4A,B;  $p < .05$ ). Paeoniflorin inhibited LPS-induced cell apoptosis and nuclear condensation, and paeoniflorin alone did not affect Schwann cell viability (Figure 4A,B;  $p < .05$ ). As for the mRNA level, LPS reduced the expression levels of Bcl-2 and Bcl-xl and increased the levels of IL1 $\beta$ , IL6, and TNF- $\alpha$  (Figure 4C;  $p < .05$ ). Paeoniflorin reduced the elevated expression of IL1 $\beta$ , IL6, and TNF- $\alpha$  and enhanced the decreased levels of Bcl-2 and Bcl-xl (Figure 4C;  $p < .05$ ). Paeoniflorin alone did not impact Schwann cells (Figure 4C;  $p < .05$ ).

### 3.9 | Paeoniflorin reduces the expression of apoptotic proteins and inhibits the nuclear translocation of NF-κB

The expression levels of apoptotic proteins, including cleaved-caspase3, caspase3, and cleaved-caspase7 (Figure 4D), were higher in the LPS group than in the other groups ( $p < .05$ ). Paeoniflorin reduced the levels of cleaved caspase3, caspase3, and cleaved-caspase7 and restored the expression of cleaved-caspase3 and cleaved-caspase7 to normal levels ( $p < .05$ ). Additionally, LPS increased the levels of TLR4 and p-NF-κB and increased the nuclear translocation of NF-κB, while paeoniflorin reversed these effects. Furthermore, paeoniflorin alone increased the expression of caspase3 only in Schwann cells (Figure 4E,  $p < .05$ ).

## 4 | DISCUSSION

In this study, we revealed that rats in the CCI group were more sensitive to mechanical, hot, and cold stimuli than those in the sham operation group, a finding that is consistent with those of previous study findings (Liu, Cheng, Ma, & Zhou, 2020; Zhang et al., 2020; J. Zhou et al., 2016; J. Zhou et al., 2017). And paeoniflorin can relieve chronic sciatica. The original and major findings are as follows: (a) paeoniflorin and mecobalamin effectively relieved neuralgia without exerting liver or kidney toxicity; (b) paeoniflorin promoted sciatic nerve repair by promoting the proliferation of Schwann cells; (c) inhibition of the TLR4/NF-κB signaling pathway reversed Schwann cell apoptosis induced by LPS in the inflammatory environment; and (d) paeoniflorin inhibited Schwann cell apoptosis by inhibiting the TLR4/NF-κB pathway in an inflammatory environment.

Behavioral tests were adopted to evaluate the chronic neuropathic pain model. After CCI operations, we observed that CCI rats exhibited cold, mechanical, and thermal hyperalgesia since the fourth day after the operation, indicating that CCI model was successful, which was consistent with our previous research results (B. Yang et al., 2021; Zhang et al., 2020). Moreover, we evaluated the



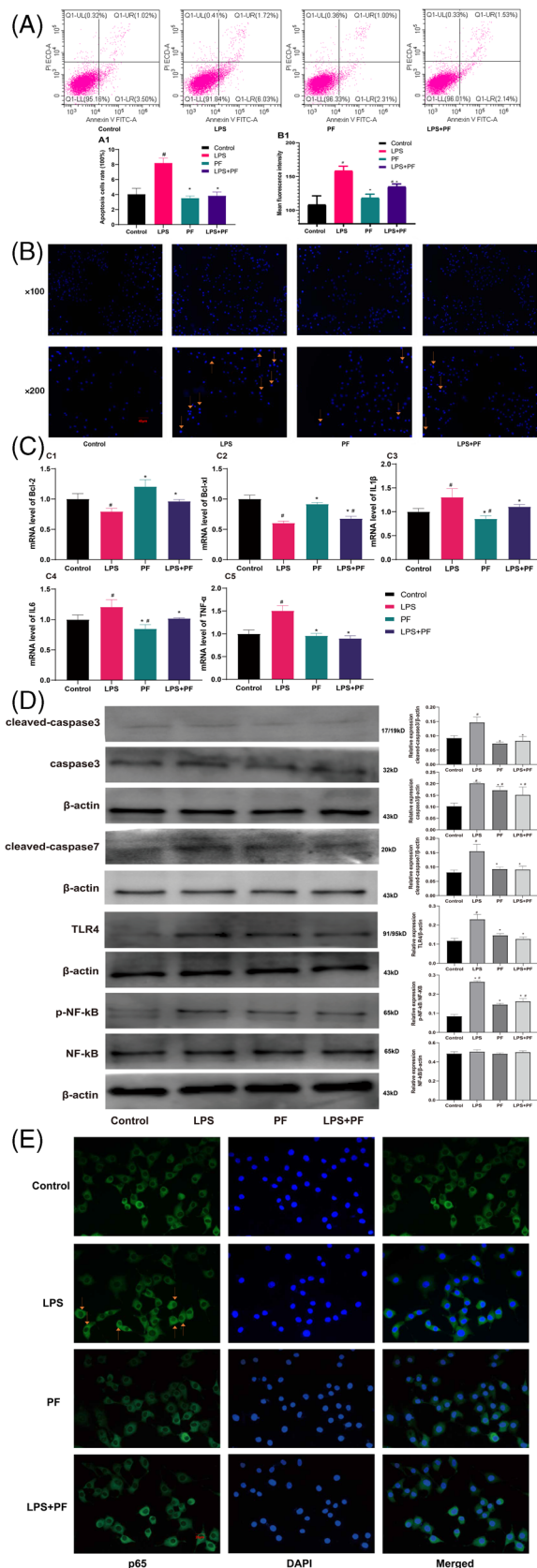


**FIGURE 4** Flow cytometry, Hoechst staining, and apoptosis-related mRNA and proteins levels. Flow cytometry (A), nuclear apoptosis (B), mRNA levels (C), related protein levels (D), and nuclear translocation of NF-kB (E). #Compared with the sham operation group and others. \*Compared with the CCI group and others.  $n = 3$

therapeutic effect of paeoniflorin through behavior tests. Paeoniflorin relieved neuropathic pain but did not normalize sensitivity from the fourth day to the 21st day. The results showed not well functional recovery for the constricted sciatic nerves in paeoniflorin group.

Analysis of the serum levels of inflammatory factors showed that CCI led to higher expression levels of inflammatory factors, including IL1 $\beta$ , TNF- $\alpha$ , IL6, CRP, and LPS, and decreased the levels of IL10. IL1 $\beta$ , TNF- $\alpha$ , IL6, CRP, and LPS can activate the immune system, while IL10 inhibits leukocyte activation and function, thus inhibiting increases in the levels of inflammatory cytokines, preventing host damage and maintaining the integrity of tissue function (Sun, Wu, Zhang, & Ni, 2021). Paeoniflorin has an antiinflammatory effect, as it reduces the levels of inflammatory factors in the spinal cord (Liu et al., 2020; J. Zhou et al., 2016, 2017). The levels of pain and inflammation are positively correlated (Lim et al., 2020). In this study, rats with higher serum levels of inflammatory factors were more sensitive to mechanical, hot, and cold stimuli, which were content with previous studies (Zhang et al., 2020). The effect of pain relief is associated with reductions in inflammatory factor levels.

Nerve damage can lead to nerve cell apoptosis. Compression with silk sutures continuously causes inflammation, leading to the persistent upregulation of the expression of multiple genes involved in neuronal apoptosis. S100 $\beta$  is a marker of Schwann cells (Choi et al., 2021), which secrete neurotrophic factors and provide structural support and guidance to promote nerve regeneration (Castro et al., 2020). B-cl-2 family members are major regulators of the apoptotic process in mammalian cells (Kale, Osterlund, & Andrews, 2018). In the normal sciatic nerve, Bcl-2 and S100 $\beta$  are distributed in the myelin sheath, thus allowing the tissue structure of the nerve to be observed. After CCI operations, Bcl-2 and S100 $\beta$  were showed disordered distribution. Additionally, Bcl-2 and S100 $\beta$  were expressed at lower levels in the CCI group than in the other groups, indicating that the CCI-affected cells underwent apoptosis, which was restored by treatment with paeoniflorin. Caspase3 is closely related to apoptosis (Beroske, Van den Wyngaert, Stroobants, Van der Veken, & Elvas, 2021), and its expression in the CCI group was higher than that in the other groups, which was reversed by treatment with paeoniflorin. CCI disrupted the nerve structure, altering the distribution of S100 $\beta$  and Bcl-2, while paeoniflorin restored the nerve structure, indicating that paeoniflorin had a neuroprotective effect (X. Yang et al., 2016). Additionally, S100 $\beta$  was expressed at the highest level in the sham operation group and at the lowest level in the CCI group, indicating that CCI operation decreased the number of Schwann cells. Given that the localization of S100 $\beta$  was the same as that of Bcl-2 and caspase3 and that the changes in S100 $\beta$  and Bcl-2 expression were the same, we speculate that Schwann cell proliferation promotes sciatic nerve injury repair.

The TLR4 inhibitor (TAK-242) and NF-kB inhibitor (JSH23) suppressed LPS-induced nuclear apoptosis by decreasing the levels of caspase3, cleaved-caspase3, and cleaved-caspase7 and increasing the mRNA levels of Bcl-2 and Bcl-xl in Schwann cells (RSC96). TAK-242 reduced the expression of p-NF-kB, while JSH23 did not decrease the

level of TLR4, which indicates that TLR4 regulates the phosphorylation of NF- $\kappa$ B. LPS induces Schwann cell apoptosis via the TLR4/NF- $\kappa$ B pathway. And paeoniflorin attenuated LPS-induced Schwann cell apoptosis by decreasing the levels of TLR4, p-NF- $\kappa$ B, caspase3, cleaved-caspase3, and cleaved-caspase7 and increasing the mRNA levels of Bcl-2 and Bcl-xl. Additionally, paeoniflorin reduced the mRNA levels of IL1 $\beta$ , IL6, and TNF- $\alpha$ . These data were consistent with the results of the animal experiments. Thus, paeoniflorin reduces Schwann cell apoptosis and inflammatory infiltration to promote the repair of the injured sciatic nerve.

Given that paeoniflorin inhibited the levels of inflammatory factors and promote nerve repair via the TLR4/NF- $\kappa$ B pathway, and that paeoniflorin had an analgesic effect, paeoniflorin can target nerve injuries and might represent a clinical medicine in the future.

## 5 | CONCLUSION

Paeoniflorin can relieve chronic sciatica in CCI rats and promote the repair of the injured sciatic nerve by reducing the levels of inflammatory factors and Schwann cell apoptosis through the TLR4/NF- $\kappa$ B pathway.

## ACKNOWLEDGMENTS

This study was supported by the National Natural Science Foundation of China (Grant No. 81874404), TCM Research Project of Guangdong Provincial Bureau of TCM (Grant No. 20222171), and Guangzhou TCM and Integrated Traditional Chinese and Western Medicine Science and Technology Project (Grant No. 202185151002).

## CONFLICT OF INTEREST

The authors declare no conflicts of interest.


## AUTHOR CONTRIBUTIONS

Di Zhang, Shiquan Chang, Xin Li, Guoping Zhao contributed substantially to the experimental design, data analysis and experimental procedures. Huimei Shi, Bei Jing, Zhenni Chen, Yi Lin, Yachun Zheng, Guoqiang Qian, and Yuwei Pan assisted with the English writing. Thank Yixuan Li for her valuable comments on statistical analysis.

## DATA AVAILABILITY STATEMENT

The data used to support the findings of this study are available from the corresponding author upon request.

## ORCID

Di Zhang  <https://orcid.org/0000-0001-9134-6573>  
 Shiquan Chang  <https://orcid.org/0000-0003-3888-9282>  
 Xin Li  <https://orcid.org/0000-0003-1594-2378>  
 Huimei Shi  <https://orcid.org/0000-0001-9026-5149>  
 Bei Jing  <https://orcid.org/0000-0002-8208-2323>  
 Zhenni Chen  <https://orcid.org/0000-0001-8040-8927>  
 Yachun Zheng  <https://orcid.org/0000-0003-0885-8258>  
 Guoqiang Qian  <https://orcid.org/0000-0003-3036-1512>

Yuwei Pan  <https://orcid.org/0000-0002-3670-9877>

Guoping Zhao  <https://orcid.org/0000-0002-5577-2329>

## REFERENCES

- Beroske, L., Van den Wyngaert, T., Stroobants, S., Van der Veken, P., & Elvas, F. (2021). Molecular imaging of apoptosis: The case of caspase-3 radiotracers. *International Journal of Molecular Sciences*, 22(8), 3948. <https://doi.org/10.3390/ijms22083948>
- Castro, R., Taetzsch, T., Vaughan, S. K., Godbe, K., Chappell, J., Settlage, R. E., & Valdez, G. (2020). Specific labeling of synaptic schwann cells reveals unique cellular and molecular features. *eLife*, 9, e56935. <https://doi.org/10.7554/eLife.56935>
- Chen, Q., Liu, Q., Zhang, Y., Li, S., & Yi, S. (2021). Leukemia inhibitory factor regulates Schwann cell proliferation and migration and affects peripheral nerve regeneration. *Cell Death & Disease*, 12(5), 417. <https://doi.org/10.1038/s41419-021-03706-8>
- Chen, Y. T., Wang, C. C., Cheng, C. P., Liu, F. C., Lee, C. H., Lee, H. S., & Peng, Y. J. (2021). Interleukin-26 has synergistic catabolic effects with palmitate in human articular chondrocytes via the TLR4-ERK1/2-c-Jun signaling pathway. *Cells*, 10(9), 2500. <https://doi.org/10.3390/cells10092500>
- Choi, S. J., Park, S. Y., Shin, Y. H., Heo, S. H., Kim, K. H., Lee, H. I., & Kim, J. K. (2021). Mesenchymal stem cells derived from Wharton's jelly can differentiate into Schwann cell-like cells and promote peripheral nerve regeneration in acellular nerve grafts. *Tissue Engineering and Regenerative Medicine*, 18(3), 467–478. <https://doi.org/10.1007/s13770-020-00329-6>
- Gonzalez-Perez, F., Hernandez, J., Heimann, C., Phillips, J. B., Udina, E., & Navarro, X. (2018). Schwann cells and mesenchymal stem cells in laminin- or fibronectin-aligned matrices and regeneration across a critical size defect of 15 mm in the rat sciatic nerve. *Journal of Neurosurgery: Spine*, 28(1), 109–118. <https://doi.org/10.3171/2017.5.Spine161100>
- Guo, Q., Mizuno, K., Okuyama, K., Lin, N., Zhang, Y., Hayashi, H., ... Sato, T. (2020). Antineuropathic pain actions of Wu-tou decoction resulted from the increase of neurotrophic factor and decrease of CCR5 expression in primary rat glial cells. *Biomedicine & Pharmacotherapy*, 123, 109812. <https://doi.org/10.1016/j.biopha.2020.109812>
- He, D. Y., & Dai, S. M. (2011). Anti-inflammatory and immunomodulatory effects of *Paeonia lactiflora* Pall., a traditional chinese herbal medicine. *Frontiers in Pharmacology*, 2, 10. <https://doi.org/10.3389/fphar.2011.00010>
- Institute of Laboratory Animal Resources (U.S.). Committee on Care and Use of Laboratory Animals. Guide for the care and use of laboratory animals. NIH publication. Bethesda, MD: U.S. Department of Health and Human Services, Public Health Service: Volumes
- Kale, J., Osterlund, E. J., & Andrews, D. W. (2018). BCL-2 family proteins: Changing partners in the dance towards death. *Cell Death & Differentiation*, 25(1), 65–80. <https://doi.org/10.1038/cdd.2017.186>
- Kou, Y. H., Yu, F., Yuan, Y. S., Niu, S. P., Han, N., Zhang, Y. J., ... Jiang, B. G. (2020). Effects of NP-1 on proliferation, migration, and apoptosis of Schwann cell line RSC96 through the NF- $\kappa$ B signaling pathway. *American Journal of Translational Research*, 12(8), 4127–4140.
- Lim, Y. Z., Wang, Y. Y., Cicutini, F. M., Hughes, H. J., Chou, L. S., Urquhart, D. M., ... Hussain, S. M. (2020). Association between inflammatory biomarkers and nonspecific low back pain a systematic review. *The Clinical Journal of Pain*, 36(5), 379–389. <https://doi.org/10.1097/Ajp.0000000000000810>
- Liu, P., Cheng, J., Ma, S., & Zhou, J. (2020). Paeoniflorin attenuates chronic constriction injury-induced neuropathic pain by suppressing spinal NLRP3 inflammasome activation. *Inflammopharmacology*, 28(6), 1495–1508. <https://doi.org/10.1007/s10787-020-00737-z>
- Livak, K. J., & Schmittgen, T. D. (2001). Analysis of relative gene expression data using real-time quantitative PCR and the 2<sup>- $\Delta\Delta$ CT</sup> Method. *Methods*, 25(4), 402–408. <https://doi.org/10.1006/meth.2001.1262>

- Ma, Z., Chu, L., Liu, H., Li, J., Zhang, Y., Liu, W., ... Gao, Y. (2016). Paeoniflorin alleviates non-alcoholic steatohepatitis in rats: Involvement with the ROCK/NF-kappaB pathway. *International Immunopharmacology*, 38, 377–384. <https://doi.org/10.1016/j.intimp.2016.06.023>
- Nair, A. B., & Jacob, S. (2016). A simple practice guide for dose conversion between animals and human. *Journal of Basic and Clinical Pharmacy*, 7(2), 27–31. <https://doi.org/10.4103/0976-0105.177703>
- Pichini, S., Solimini, R., Berretta, P., Pacifici, R., & Busardo, F. P. (2018). Acute intoxications and fatalities from illicit fentanyl and analogues: An update. *Therapeutic Drug Monitoring*, 40(1), 38–51. <https://doi.org/10.1097/FTD.0000000000000465>
- Sun, H., Wu, Y. Z., Zhang, Y., & Ni, B. (2021). IL-10-producing ILCs: Molecular mechanisms and disease relevance. *Frontiers in Immunology*, 12, 650200. <https://doi.org/10.3389/fimmu.2021.650200>
- Tao, T., Zheng, H., Yang, L. Y., Guo, X. W., Zhang, J., Lv, C., ... Shi, D. S. (2017). Paeoniflorin attenuates neuropathic pain through the regulation of Sirt1 in rats. *International Journal of Clinical and Experimental Medicine*, 10(3), 4678–4686.
- Treede, R. D., Jensen, T. S., Campbell, J. N., Cruccu, G., Dostrovsky, J. O., Griffin, J. W., ... Serra, J. (2008). Neuropathic pain: Redefinition and a grading system for clinical and research purposes. *Neurology*, 70(18), 1630–1635. <https://doi.org/10.1212/01.wnl.0000282763.29778.59>
- Truini, A., Garcia-Larrea, L., & Cruccu, G. (2013). Reappraising neuropathic pain in humans—how symptoms help disclose mechanisms. *Nature Reviews Neurology*, 9(10), 572–582. <https://doi.org/10.1038/nrneurol.2013.180>
- Yang, B., Ma, S., Zhang, C., Sun, J., Zhang, D., Chang, S., ... Zhao, G. (2021). Higenamine attenuates neuropathic pain by inhibition of NOX2/ROS/TRP/P38 mitogen-activated protein kinase/NF-kB signaling pathway. *Frontiers in Pharmacology*, 12, 716684. <https://doi.org/10.3389/fphar.2021.716684>
- Yang, X., Yao, W., Shi, H., Liu, H., Li, Y., Gao, Y., ... Xu, L. (2016). Paeoniflorin protects Schwann cells against high glucose induced oxidative injury by activating Nrf2/ARE pathway and inhibiting apoptosis. *Journal of Ethnopharmacology*, 185, 361–369. <https://doi.org/10.1016/j.jep.2016.03.031>
- Yoon, C., Wook, Y. Y., Sik, N. H., Ho, K. S., & Mo, C. J. (1994). Behavioral signs of ongoing pain and cold allodynia in a rat model of neuropathic pain. *Pain*, 59(3), 369–376. [https://doi.org/10.1016/0304-3959\(94\)90023-X](https://doi.org/10.1016/0304-3959(94)90023-X)
- Yuan, N., Gong, L., Tang, K., He, L., Hao, W., Li, X., ... Chen, J. (2020). An integrated pharmacology-based analysis for antidepressant mechanism of Chinese Herbal Formula Xiao-Yao-San. *Frontiers in Pharmacology*, 11, 284. <https://doi.org/10.3389/fphar.2020.00284>
- Zhai, G. L., Liang, W. F., & Xu, Y. J. (2021). High expression of lysophosphatidic acid induces nerve injury in LSS patients via AKT mediated NF-kB p65 pathway. *Frontiers in Pharmacology*, 12, 641435. <https://doi.org/10.3389/fphar.2021.641435>
- Zhang, D., Chen, D., Ma, S. S., Bian, W. Y., Xie, F., Huang, M. N., ... Zhao, G. (2019). Effect of Danggui Sini decoction on the behaviour and dorsal root ganglion TRP channel of neuropathic pain in CCI rats. *Indian Journal of Pharmaceutical Sciences*, 81(5), 922–932. <https://doi.org/10.36468/pharmaceutical-sciences.587>
- Zhang, D., Sun, J., Chang, S., Li, X., Shi, H., Jing, B., ... Zhao, G. (2021). Protective effect of 18β-glycyrrhetic acid against H<sub>2</sub>O<sub>2</sub>-induced injury in Schwann cells based on network pharmacology and experimental validation. *Experimental and Therapeutic Medicine*, 22(5), 1241. <https://doi.org/10.3892/etm.2021.10676>
- Zhang, D., Sun, J., Yang, B., Ma, S., Zhang, C., & Zhao, G. (2020). Therapeutic effect of *Tetrapanax papyriferus* and hederagenin on chronic neuropathic pain of chronic constriction injury of sciatic nerve rats based on KEGG pathway prediction and experimental verification. *Evidence-Based Complementary and Alternative Medicine*, 2020, 2545806. <https://doi.org/10.1155/2020/2545806>
- Zhang, D., Yang, B., Chang, S. Q., Ma, S. S., Sun, J. X., Yi, L., ... Zhao, G. P. (2021). Protective effect of paeoniflorin on H<sub>2</sub>O<sub>2</sub> induced Schwann cells injury based on network pharmacology and experimental validation. *Chinese Journal of Natural Medicines*, 19(2), 90–99. [https://doi.org/10.1016/S1875-5364\(21\)60010-9](https://doi.org/10.1016/S1875-5364(21)60010-9)
- Zhou, D., Zhang, S., Hu, L., Gu, Y. F., Cai, Y., Wu, D., ... Zhang, G. Q. (2019). Inhibition of apoptosis signal-regulating kinase by paeoniflorin attenuates neuroinflammation and ameliorates neuropathic pain. *Journal of Neuroinflammation*, 16(1), 83. <https://doi.org/10.1186/s12974-019-1476-6>
- Zhou, J., Wang, J., Li, W., Wang, C., Wu, L., & Zhang, J. (2017). Paeoniflorin attenuates the neuroinflammatory response in a rat model of chronic constriction injury. *Molecular Medicine Reports*, 15(5), 3179–3185. <https://doi.org/10.3892/mmr.2017.6371>
- Zhou, J., Wang, L., Wang, J., Wang, C., Yang, Z., Wang, C., ... Zhang, J. (2016). Paeoniflorin and albiflorin attenuate neuropathic pain via MAPK pathway in chronic constriction injury rats. *Evidence-Based Complementary and Alternative Medicine*, 2016, 8082753. <https://doi.org/10.1155/2016/8082753>

**How to cite this article:** Zhang, D., Chang, S., Li, X., Shi, H., Jing, B., Chen, Z., Lin, Y., Zheng, Y., Qian, G., Pan, Y., & Zhao, G. (2022). Therapeutic effect of paeoniflorin on chronic constriction injury of the sciatic nerve via the inhibition of Schwann cell apoptosis. *Phytotherapy Research*, 36(6), 2572–2582. <https://doi.org/10.1002/ptr.7472>